



Solitary Waves in Nonlinear Beam Equations: Stability, Fission and Fusion

A. R. CHAMPNEYS

Department of Engineering Mathematics, University of Bristol, Bristol BS8 1TR, U.K.

P. J. McKENNA

Department of Mathematics, University of Connecticut, Storrs, CT 06268, U.S.A.

P. A. ZEGELING

Mathematical Institute, University of Utrecht, 3584 CD Utrecht, The Netherlands

(Received: 8 September 1998; accepted: 22 June 1999)

Abstract. We continue work by the second author and co-workers on solitary wave solutions of nonlinear beam equations and their stability and interaction properties. The equations are partial differential equations that are fourth-order in space and second-order in time. First, we highlight similarities between the intricate structure of solitary wave solutions for two different nonlinearities; a piecewise-linear term versus an exponential approximation to this nonlinearity which was shown in earlier work to possess remarkably stable solitary waves. Second, we compare two different numerical methods for solving the time dependent problem. One uses a fixed grid discretization and the other a moving mesh method. We use these methods to shed light on the nonlinear dynamics of the solitary waves. Early work has reported how even quite complex solitary waves appear stable, and that stable waves appear to interact like solitons. Here we show two further effects. The first effect is that large complex waves can, as a result of roundoff error, spontaneously decompose into two simpler waves, a process we call *fission*. The second is the fusion of two stable waves into another plus a small amount of radiation.

Keywords: Solitary waves, nonlinear dynamics, beam equation, wave interaction, moving mesh method.

1. Introduction

Historical accounts of travelling wave behaviour in the Golden Gate Bridge in San Francisco motivated McKenna and Walter [21] to study travelling wave solutions in a nonlinear beam equation

$$u_{tt} + u_{xxxx} + f(u) = 0, \quad (1)$$

where the highly idealized nonlinearity f is chosen to model the effect that the cable holds the beam up but the constant force of gravity holds it down. (See also [17] for some general issues surrounding using such simple nonlinear beam equations as suspension-bridge models.) This led to the beam equation with restoring force of the general shape

$$f(u) = (u^+ - 1), \quad \text{where } u^+ = \begin{cases} u, & u > 0, \\ 0, & u < 0. \end{cases} \quad (2)$$

Here the function $u(x, t)$ represents the displacement of the beam from the unloaded state. The natural equilibrium is at $u \equiv 1$ and solutions of the form $u(x, t) = 1 + y(x - ct)$ were found explicitly for the piecewise nonlinearity. Such solutions satisfy the ODE

$$y'''' + c^2 y'' + f(y + 1) = 0, \quad (3)$$

where a prime denotes differentiation with respect to $\xi = (x - ct)$.

Motivated by the observations on the Golden Gate, a prime concern is the possible existence and stability of solitary wave solutions of Equation (1). These correspond to homoclinic-to-zero solutions of Equation (3), i.e. $(y, y', y'', y''') \rightarrow 0$ as $\xi \rightarrow \infty$. Using the piecewise-linear nature of the restoring force (2), McKenna and Walter [21] were able to construct explicitly several homoclinic solutions for a range of values of $c^2 < 2$. Using Mountain-Pass variational methods, Chen and McKenna [9] showed that for a class of f including Equation (2) there exists at least one homoclinic solution for all $0 < c^2 < 2$. More recently, Champneys and McKenna [6] provided a partial classification of these solutions (see Section 3 below) and showed that there are infinitely many homoclinic solutions of multi-trough type for $0 < c_{\min}^2 < c < c_{\max}^2 < 2$.

The piecewise-linear model has at least two limitations. First, it oversimplifies the nonlinearity of the physical situation, not allowing nonlinear effects until the deflection is quite large. Second, the absence of smoothness may lead to numerical difficulties, Equation (1). So, Chen and McKenna [9, 10], also studied the analytic nonlinearity

$$f(u) = \exp(u - 1) - 1. \quad (4)$$

They found numerical evidence for some curious stability and interaction properties of solitary waves, that lead them to conjecture that Equation (1) is completely integrable since certain of the solutions were behaving like solitons although there was no qualitative support for this conjecture. (See also [22] for existence of complex periodic waves of Equation (1) with smooth f , Equation (4).)

In what follows we shall consider several different versions of the nonlinearity with the same qualitative features, including the smooth function

$$f(u) = \frac{\sqrt{1 + \varepsilon} \left(u + \sqrt{u^2 + \varepsilon} \right)}{1 + \sqrt{1 + \varepsilon}} - \sqrt{1 + \varepsilon}, \quad (5)$$

where $\varepsilon > 0$ is a tunable parameter. Such a function has the same equilibrium at $u = 1$ and the same linearization there. Moreover it tends to Equation (2) both in the limits $|u| \rightarrow \infty$ and $\varepsilon \rightarrow 0$.

Note that ODEs of the form (3) arise from steady states or travelling waves of PDEs in other contexts, for example in water-waves, buckling problems, models for pattern formation. For a review, see [4, 5] and references therein. Typical nonlinearities arising in those problems include $f = y - y^2$, $y + ay^2 + by^3$ etc. Also Equation (3) with the very nonlinearity (2) has been used to describe deflections of railroad tracks and undersea oil pipelines [14, 19].

Before proceeding, let us notice some basic facts about Equation (3), assuming $f'(y)|_0 = 1$ as it is for all the f 's under consideration. First, it is reversible, that is invariant under the transformation

$$R : (\xi, y, y', y'', y''') \rightarrow (-\xi, y, -y', y'', -y'''). \quad (6)$$

Since Equation (3) is autonomous, this invariance means that all solutions $y(\xi)$ that intersect the *symmetric section* $\mathcal{S} := \{y' = y''' = 0\}$ will be even about that point. Second, Equation (3) is conservative with first integral

$$H = y'''y' + \frac{c^2(y')^2}{2} - \frac{(y'')^2}{2} + \int f(s + 1) ds, \quad (7)$$

and a co-ordinate transformation exists to express it as a Hamiltonian system in \mathbb{R}^4 . Finally, when looking for homoclinic solutions to $y = 0$, we need to look at the linearization there. From the characteristic equation, observe that when $c^2 < 2$, the eigenvalues form a complex quadruple $\pm\lambda \pm i\omega$ where $\lambda \rightarrow 0$ as $c^2 \rightarrow 2$. For $c^2 > 2$, the eigenvalues are pure imaginary. Hence, independent of the precise form of f , we should only expect to see homoclinic solutions when the origin is hyperbolic, that is $0 < c^2 < 2$.

The purpose of this paper is to provide further understanding of the existence, stability and interaction properties of solitary wave solutions to Equation (1). In particular, we want to examine more carefully any soliton-like behaviour and see whether the precise analytic form of f is important in what is observed. The techniques of analysis will be largely numerical, but we shall seek to explain the results in terms of analytical information already known about PDEs of the form (2).

The rest of the paper is outlined as follows. Section 2 describes three different numerical techniques for the computation of solitary wave solutions using Equation (3) and a fixed and a moving mesh method for time integration of solutions to the PDE. Section 3 then recalls a categorization of homoclinic solutions to Equation (3). There are known to be infinitely many of these for various nonlinear functions f , and we show bifurcation diagrams with c of some of the simplest solutions. Section 4 then contains an in depth investigation of the stability and interaction properties of a representative sample of these solutions. Primarily the smooth, exponential nonlinearity (4) is used, but the results are also compared with those for other nonlinearities. Finally, Section 5 draws conclusions, draws parallels with known numerical and analytical results for related systems and suggests avenues for future research.

2. Numerical Methods

There are two different problems to be dealt with in investigating the properties of these waves. First, we have to find them. Finding homoclinic solutions of Equation (3) is not a trivial task but there is now considerable understanding of how to do this. This shall be the subject of the first subsection.

Having found a travelling wave solution, our next task is to see how they behave as solutions of the partial differential equation (2). Naturally, this involves solving the initial value problem numerically, preferably for as long a time as possible. Early efforts at solving this initial value problem used an explicit finite difference method. This had a number of advantages. First, it was easy to program. Second, because of the local nature of the algorithm, it was possible to include many different boundary conditions. However, it had one significant disadvantage; the restrictions related to stability made it difficult to refine the mesh size so as to check the accuracy of the results.

In this paper, we have again used the explicit method, especially for long-time results. This is described in Section 2.2. As always, when dealing with numerical results, one has to worry about whether these results are a product of the algorithm. To partially avoid this problem and obtain confirmation of our results, we have used a more sophisticated method which allows for considerably better control of numerical error. This adaptive grid technique is described in Section 2.3.

2.1. LOCATION OF SOLITARY WAVES

A shooting method for finding symmetric solutions which are homoclinic to symmetric equilibria in reversible systems was presented in [8], where it was also applied to Equation (3) with $f = y - y^2$. The basic idea is to truncate the two-point boundary-value problem to a finite ξ interval with left-hand boundary conditions that place the solution in the linearized unstable manifold of the equilibrium. An angle co-ordinate and the unknown length of the truncated interval are then used as shooting parameters in order to satisfy a right-hand boundary condition that the solution lies in the symmetric section \mathcal{S} of the reversibility. This shooting problem can then be solved using Newton's method allied to an accurate initial-value solver, with the Jacobian calculated via the variational equation of the ODE. Other shooting methods can be used to find non-symmetric solutions. Also, a variant of this approach can be coded into a continuation package, for this work AUTO [12].

Using these methods it is possible to accurately locate large families of homoclinic solutions to the origin of Equation (3) for whatever f and to continue these solutions as c varies. The results can be used as initial data for the time integrations of Equation (1). As the reader will see, the solutions range from simple primary waves to quite complicated multi-noded structures.

2.2. A FINITE DIFFERENCE METHOD

We analyse the solution of the initial value problem for Equation (1) on the finite interval $[-L, L]$, with periodic boundary conditions.

The finite difference scheme which was originally used in [9, 10] was the simplest explicit scheme with second-order accuracy. We approximate the second derivative in time with a three-point central difference, and the fourth derivative in space with a five-point central difference. This gives

$$\frac{u_m^{n+1} - 2u_m^n + u_m^{n-1}}{k^2} + \frac{u_{m+2}^n - 4u_{m+1}^n + 6u_m^n - 4u_{m-1}^n + u_{m-2}^n}{h^4} + f(u_m^n) = 0, \quad (8)$$

for $n = 1, 2, 3, \dots$ and $m = 0, 1, 2, \dots, M$, where $k = \Delta t$ is the time step, $h = \Delta x = 2L/M$, and $u_m^n = u(x_m, t_n) = u(-L + mh, nk)$. This gives the explicit scheme

$$u_m^{n+1} = 2u_m^n - u_m^{n-1} - k^2 \left[\frac{u_{m+2}^n - 4u_{m+1}^n + 6u_m^n - 4u_{m-1}^n + u_{m-2}^n}{h^4} + f(u_m^n) \right]. \quad (9)$$

Stability analysis shows that this scheme is stable if and only if $k/h^2 \leq 1/2$. The main drawback of this method is that the stability requirement makes it very difficult to obtain large-time results with a small step size.

This scheme requires two sets of initial data, at time steps 0 and 1. We use a standard Taylor series method to approximate the first time step with

$$u_m^1 = u_m^0 - ckz'_m - \frac{k^2}{2} \left[\frac{u_{m+2}^0 - 4u_{m+1}^0 + 6u_m^0 - 4u_{m-1}^0 + u_{m-2}^0}{h^4} + f(u_m^0) \right], \quad (10)$$

where $y'_m = z'(-L + mh)$.

For most of the experiments described in this paper, the boundary conditions which we use are periodic. This is the simplest way to study long time behaviour of the waves interacting

repeatedly, as long as the waves remain reasonably intact and localised. Occasionally, when not studying long-term behaviour, a non-reflecting boundary condition [9] was used.

2.3. AN ADAPTIVE MOVING-GRID METHOD

Before applying an adaptive grid method it is useful to transform the nonlinear beam equation (1) to a system of three PDEs involving first-order time-derivatives. If we define

$$v := u_t, \quad w := u_{xx}, \quad \eta := (u, v, w)^T, \quad \mathcal{F} := (0, f(u), 0)^T,$$

then PDE (1) can be re-written as

$$\eta_t = \mathcal{A}\eta_{xx} + \mathcal{B}\eta + \mathcal{F}, \quad (11)$$

where \mathcal{A} is the matrix $\begin{pmatrix} 0 & 0 & 0 \\ 0 & 0 & -1 \\ 0 & 1 & 0 \end{pmatrix}$ and \mathcal{B} the matrix $\begin{pmatrix} 0 & 1 & 0 \\ 0 & 0 & 0 \\ 0 & 0 & 0 \end{pmatrix}$. For a PDE (system) in the form (11) it is common, if we would like to use an adaptive grid method, to introduce an additional coordinate transformation from the physical domain to the computational domain:

$$\xi = \xi(x, t), \quad \tau = \tau(x, t) = t. \quad (12)$$

It is straightforward to apply this coordinate transform to Equation (11), giving

$$\eta_\tau - \frac{x_\tau}{\mathcal{J}}\eta_\xi = \frac{1}{\mathcal{J}} \left(\frac{\mathcal{A}}{\mathcal{J}}\eta_\xi \right)_\xi + \mathcal{B}\eta + \mathcal{F}, \quad (13)$$

where $\mathcal{J} = x_\xi$ is the Jacobian of (12).

To complete the system of equations (in other words: implicitly defining the coordinate transformation (12)) a so-called moving grid is used that is based on an ‘equidistribution principle’ enhanced with smoothing procedures in time and space:

$$\frac{\partial}{\partial \xi} \left[\frac{\tilde{n} + \tau_s \dot{\tilde{n}}}{\mathcal{W}} \right] = 0. \quad (14)$$

Here \tilde{n} is the non-smoothed grid point concentration and the weight function \mathcal{W} is taken as $\mathcal{W} = \sqrt{1 + \alpha(u_x)^2}$, where the parameter $\alpha \geq 0$ controls the level of adaptivity to the solution gradient $\partial u / \partial x$. The grid point concentration $n = 1/\mathcal{J}$ that is used in Equation (14) is obtained by smoothing \tilde{n} :

$$\left[I - \kappa(\kappa + 1)(\Delta\xi)^2 \frac{\partial^2}{\partial \xi^2} \right] n = \tilde{n}, \quad (15)$$

with κ the spatial smoothing parameter, I the identity operator, and $\Delta\xi$ the uniform cell-size in the ξ -direction. With $\kappa = O(1)$, rather modestly stretched space grids are obtained. The parameter τ_s in Equation (14) controls the temporal smoothness of the grid; it provides a means for suppressing grid oscillations in time. See [1, 27] for more details on the use of the grid parameters and equations like (14) and (15).

The semi-discretization of Equation (13) combined with Equation (14) together with appropriate boundary conditions gives a large system of ODEs (for the semi-discrete vectors \dot{H} and \dot{X} corresponding to the PDE variables u, v, w and x) that is solved with the stiff ODE

integrator DASSL [23]. In all the computations below using the moving mesh method we have used Dirichlet boundary conditions in u , v and w .

3. Families of Solitary Wave Solutions

Homoclinic to zero solutions to Equation (3) with nonlinearity (2), corresponding to solitary wave solutions to Equation (1) with the piecewise-linear f , were investigated exhaustively in [6]. Aside from a ‘primary’ wave, two different classes of solutions were identified, being of *multi-wiggle* or *multi-trough* type. The multi-wiggle solutions have troughs which are much deeper than that of the primary for a given $c^2 < 2$, with many oscillations in y' as y decreases to its global minimum. Since large amplitude solutions are likely to be less physically realistic in any application of Equation (1), we shall ignore these solutions in what follows. Figure 1 shows the bifurcation diagram with $c > 0$ of the primary and simplest multi-trough (also referred to in other models as *multi-pulse*) homoclinic solutions. The bifurcation diagram for $c < 0$ is identical since only c^2 appears in the Equation (3). Also only solutions for c sufficiently close to $\sqrt{2}$ are depicted. The numerical evidence suggests that all branches continue all the way to $c = 0$ (recall [9] it is proved that there is at least one solution for all $0 < c < \sqrt{2}$). However all solutions tend to infinity in this limit in the supremum norm [16], that is the $\min y(x) \rightarrow -\infty$ as $c \rightarrow 0$.

Following the notation introduced by Champneys and Toland [7] who studied Equation (3) with $f = y - y^2$, for c sufficiently small we can label the multi-trough solutions by strings of integers $\mathbf{n}(m_1, m_2, \dots, m_{n-1})$ where \mathbf{n} counts the number of troughs (approximate copies of the primary) and the m_i count the number of half-oscillations between the troughs. The insets in Figure 1 depict the profiles of the primary and the first three two-pulsed waves. Note that for this model we find no solutions with $m_i = 1$ in the notation of [7], and for the $\mathbf{2}(m)$ solutions depicted one can read off the symbol m from the nature of the midpoint of the graph of u . (The graph of each two-troughed wave is even since they are all reversible under R .)

- $m = 1(\text{mod } 4)$ corresponds to a negative maximum of $y(\xi)$,
- $m = 2(\text{mod } 4)$ corresponds to a positive maximum of y ,
- $m = 3(\text{mod } 4)$ corresponds to positive minimum, and
- $m = 0(\text{mod } 4)$ corresponds to a negative minimum.

Figure 1 also illustrates the range of c in which the simplest few solution exist. The primary and $\mathbf{2}(2)$ remain all the way to $c = \sqrt{2}$, where their $\min(y)$ tends to -1 . (Note that, given Equation (2), all homoclinic solutions must satisfy $y(\xi) > -1$, for some ξ , otherwise the equation would be completely linear.) All other solutions are observed to turn around at folds in the bifurcation diagram, which is a process by which more troughs are generated. Two cases are illustrated, the $\mathbf{2}(3)$ becoming a $\mathbf{4}(2, 3, 2)$ and the $\mathbf{2}(4)$ becoming a $\mathbf{3}(2, 2)$. Note that the graphs of the $\mathbf{2}(4)$ and $\mathbf{3}(2, 2)$ displayed for $c = 1.3$ are qualitatively similar. This is because at only a slightly greater c -value, these two branches connect. If the solutions are followed back to smaller c -values, it is found that their graph shapes are very different, the $\mathbf{3}(2, 2)$ has three deep troughs whereas the middle trough of $\mathbf{2}(4)$ remains in the vicinity of $y = 0$.

Buffoni et al. [2] computed a large sequence of branches similar to those in Figure 1, but for Equation (3) with $f = y - y^2$. The results are qualitatively similar except in two respects. First, the primary and $\mathbf{2}(2)$ solutions bifurcate from zero amplitude at $c^2 = 2$ and, second, solutions

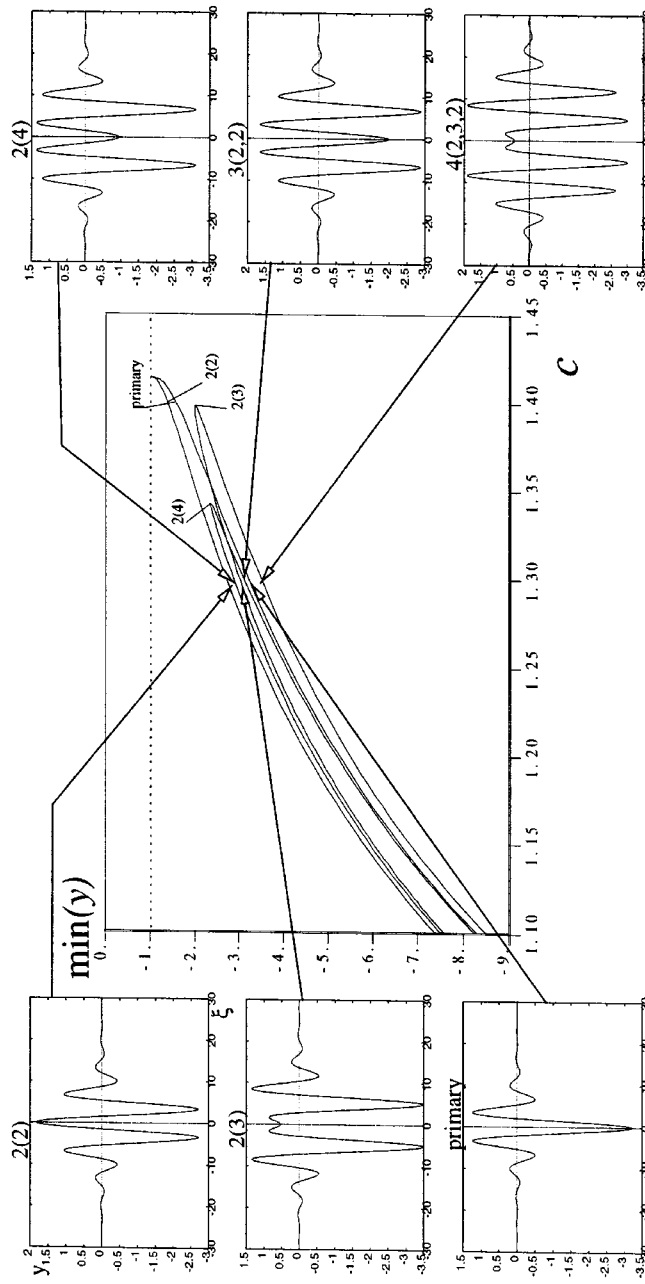


Figure 1. Homoclinic solutions to zero of the ODE (3) with (2) for c^2 close to 2. Only the primary and simplest three multi-trough solutions are depicted.

stay bounded as $c \rightarrow 0$. But the process of all other multi-trough solutions forming extra troughs in fold bifurcations was exactly the same, and a list of exclusion principles or ‘rules for coalescence’ were proposed in order to determine the labeling of solutions that are joined at the fold points. As far as we can tell, for each f under consideration here, qualitatively similar bifurcation diagrams are found for c near $\sqrt{2}$, which obey these rules.

We illustrate this similarity by showing in Figure 2 the corresponding figure to Figure 1 for the exponential nonlinearity (4). Note that there are few qualitative differences, between the two figures. The solutions for the exponential nonlinearity have slightly deeper troughs and shallower peaks. Also, as $c \rightarrow \sqrt{2}$, rather than approach a minimum value -1 , the primary and $\mathbf{2}(2)$ solutions tend to zero uniformly. This bifurcation from zero amplitude is known to be the case for the model with $f = y - y^2$. In fact, a calculation [26] shows that the results of Iooss and Perouème [15] apply the exponential nonlinearity case, thereby proving that these two solutions bifurcate. Note that for the piecewise-linear f , such a bifurcation is impossible because solutions which remain everywhere above $y = -1$ solve a completely linear system and so cannot be homoclinic.

4. Stability and Interaction Properties

This section contains most of the new results of the paper. We shall organize the results by presenting results first for the exponential nonlinearity (4), starting with some of the simplest solitary waves, followed by some results on their interaction and finally illustrating the extra complexity of waves with four large troughs. We then present evidence which suggests there is little or no qualitative differences between the three alternative forms of the restoring force $f(u)$.

4.1. STABILITY

As found in the earlier numerical results of Chen and McKenna, it would appear that the primary solitary wave solution of Equation (4) is a stable solution of the initial value problem, at least for c close to the maximum wave speed $c = \sqrt{2}$.

Two-pulse solutions $\mathbf{2}(n)$ appear to have the property that they are stable if n is odd (i.e. $uu_{xx} > 0$ at the midpoint of the wave profile, without loss of generality $x = 0$) and unstable if n is even (i.e. $u(0)u_{xx}(0) < 0$). Figure 3a shows the time evolution of the $\mathbf{2}(5)$ wave for $c = 1.1$.

Other more complex apparently stable solitary waves are depicted in Figures 3b–3d.

CONJECTURE 1. *For a range of c -values less than $\sqrt{2}$, there are infinitely many stable solitary wave solutions of Equation (4). In particular, in the notation of [7] $\mathbf{2}(2m + 1)$ waves are stable for $m = 1, 2, 3, \dots$*

4.2. FISSION OF DOUBLE-PULSE WAVES INTO STABLE ONES

The two-pulse solutions that are unstable appear to each obey the same form of instability. Figure 4 shows what happens to the $\mathbf{2}(2)$ solution for $c = 1.1$ and 1.3 . In both cases, the wave splits into two simpler waves that travel at different wave speeds. In both cases we identify the simpler waves as being primary solutions. The results presented in Figure 4b are harder to resolve with certainty. Because the smaller-amplitude primary wave travels at close to the

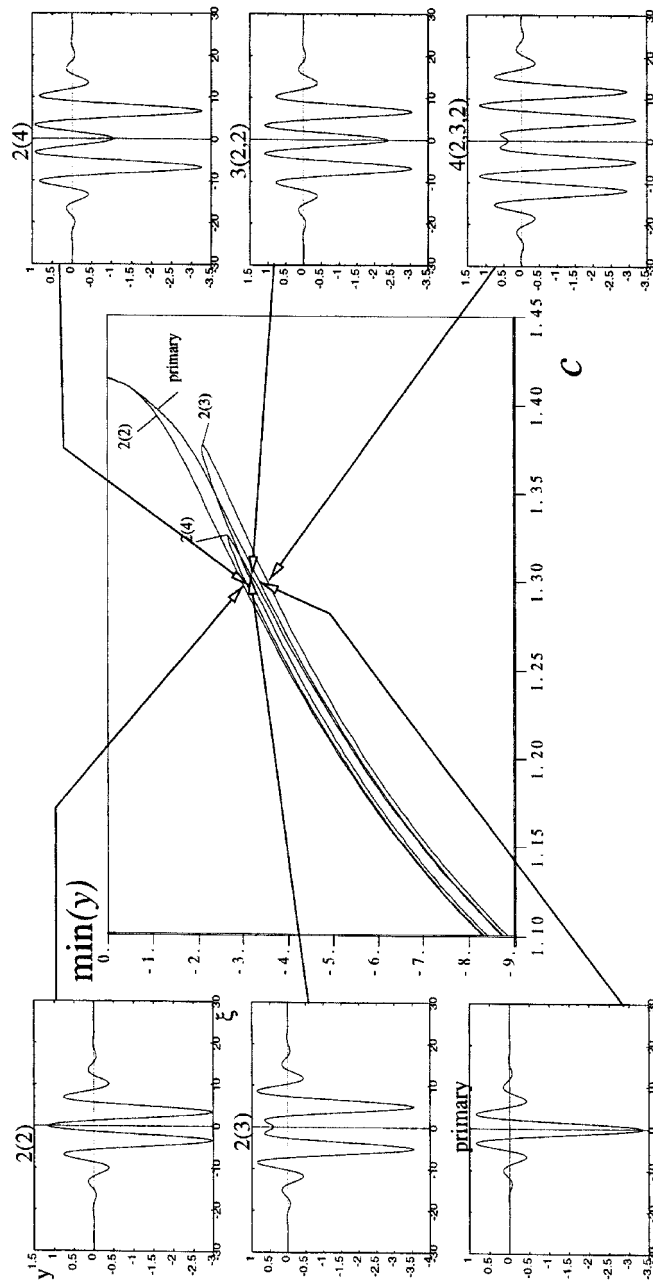


Figure 2. Analogous to Figure 1 but for the nonlinearity (4).

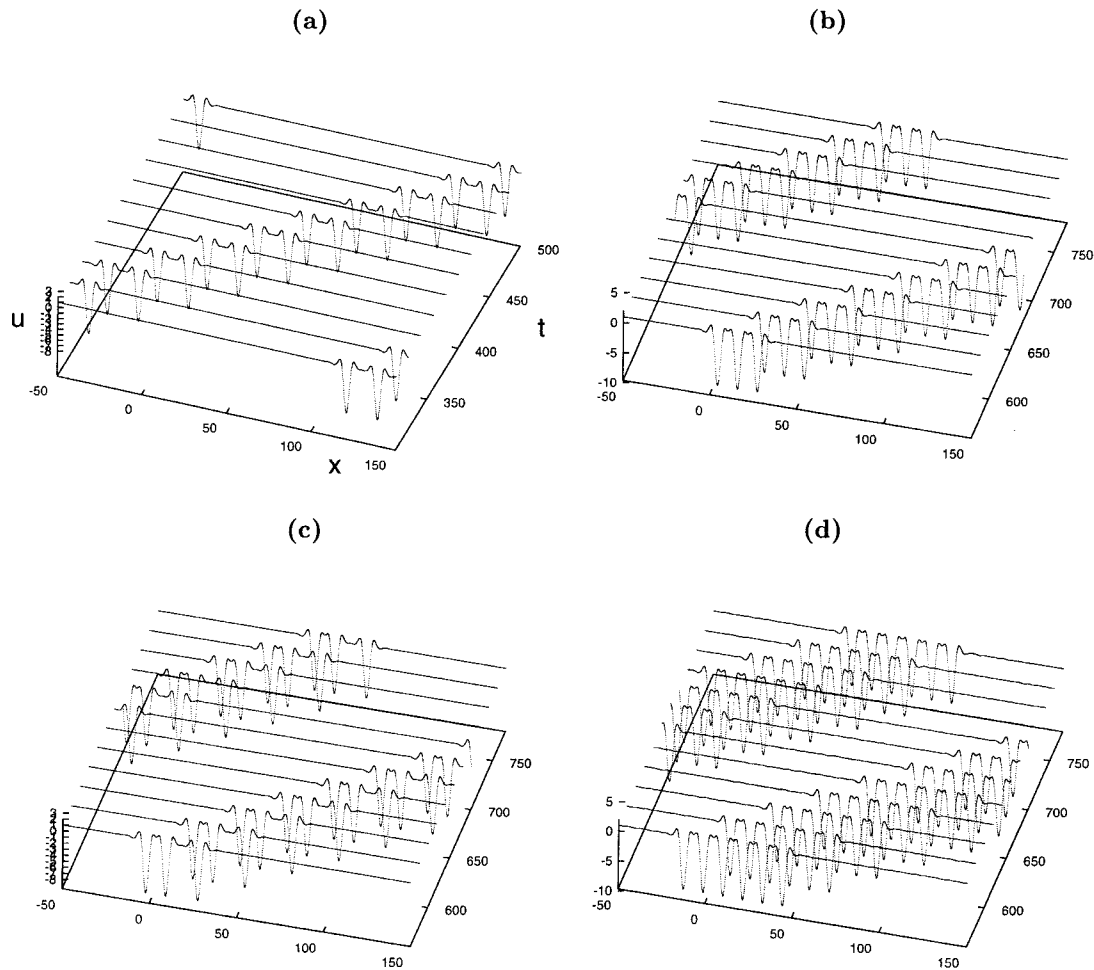


Figure 3. Simple and complicated stable solutions; numerical solutions to Equation (4) using the fixed grid method with initial conditions for $c = 1.1$ which are exact solitary waves that appear to be stable: (a) the $2(5)$; (b) the $3(3, 3)$; (c) the $3(3, 5)$ (note this is an asymmetric wave); and (d) the $6(3, 3, 3, 3, 3, 3)$. In each case the solution is plotted after a time interval which is sufficient for any transient instabilities to develop.

critical wave speed $c = \sqrt{2}$ and therefore is of small amplitude, it is hard to distinguish from radiating numerical noise. The results in Figure 4a appear cleaner. For clarity we shall henceforth restrict computations to the typical value of wave speed of initial conditions $c = 1.1$. However, all evidence suggests that the mechanism of instability is a property of branches of solutions (parameterized by wave speed) rather than of a particular solution on the branch.

The speed and amplitude of the primary waves emanating from the instability of the $2(2)$ wave were found to be repeatable using different numerical methods different error tolerances, numbers of mesh points etc. Figure 4c shows the movement of grid points using the moving grid method with exactly the same initial conditions as Figure 4a. From this graph it is possible to read off approximate values of the wave speeds of the two primary solutions born in the fission instability, viz. $c \approx 1.04$ and $c \approx 1.20$. Also, Figure 4d shows a comparison between solutions calculated using the two different numerical methods at the same time instant. Note that there is no *a priori* reason to suspect that the two methods should give the same profile,

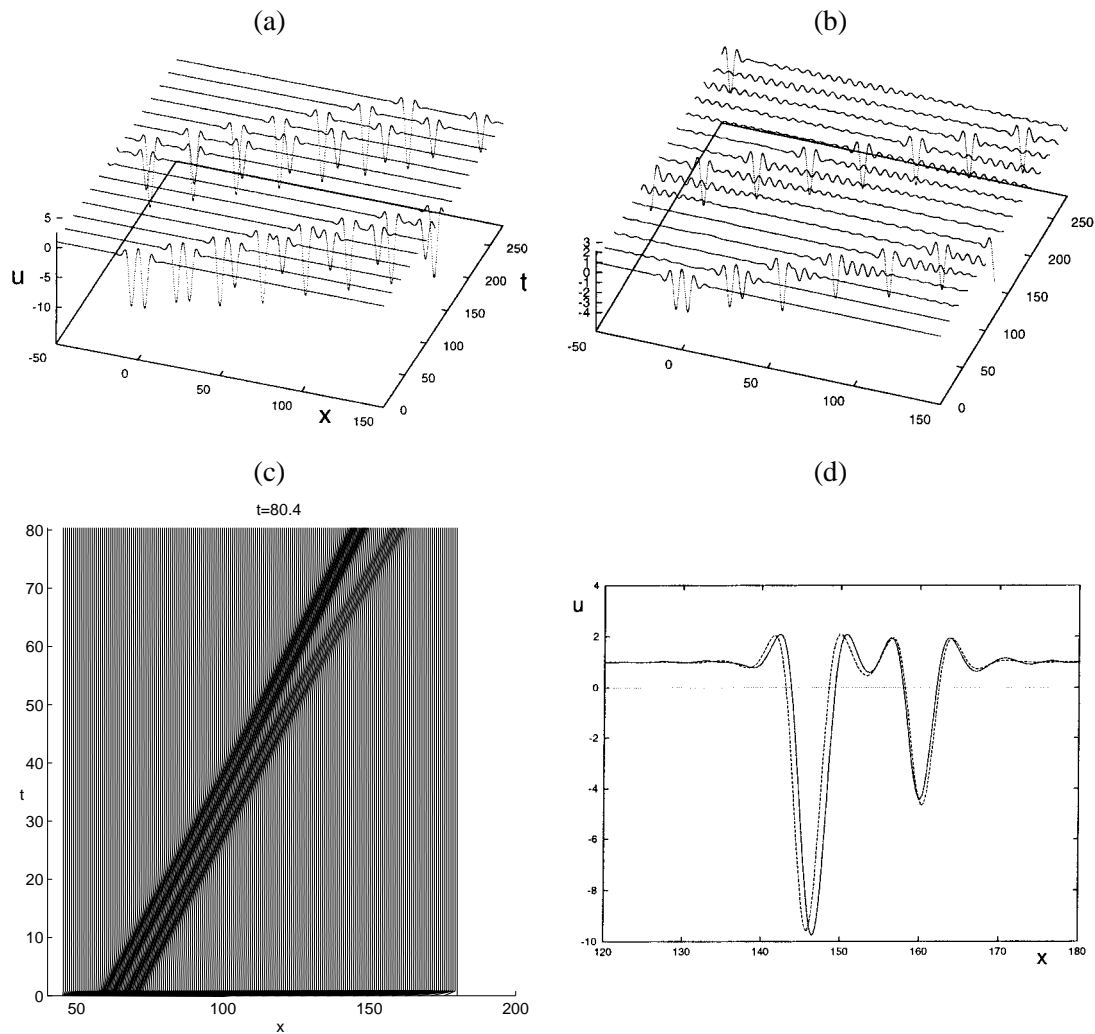


Figure 4. (a), (b) Some complicated waves spontaneously decompose into simpler ones; solutions to Equation (4) using the fixed grid method with initial conditions the $2(2)$ solitary wave for (a) $c = 1.1$ and (b) $c = 1.3$. (c) Grid from the moving-mesh method with 601 grid points using the same initial data as (a) showing fission of solitary wave $2(2)$ with $c = 1.1$ into two simpler waves with different wave speeds. (d) Comparisons between solutions at $t = 80.4$ using the fixed grid method (solid line) and the moving grid method (dashed line).

since the ‘noise’ that initiates the instability that breaks the exact $2(2)$ wave is caused only by numerical error. Therefore, the time required to reach a given separation between the two primary pulses will be a delicate function of the numerical implementation. Nevertheless we find good agreement between the two methods, which suggests that the bulk of the noise was present in the initial data. Moving mesh computations from the same initial data but with more grid points gave qualitatively similar results.

However, a new phenomenon emerged when slight modifications were made to the initial conditions or numerical implementation of the moving mesh method. This phenomenon is illustrated in Figures 5a and 5b which was run with the same initial data but a change to zero-flux conditions at a boundary that moves at the wave speed of the initial conditions. Now, the

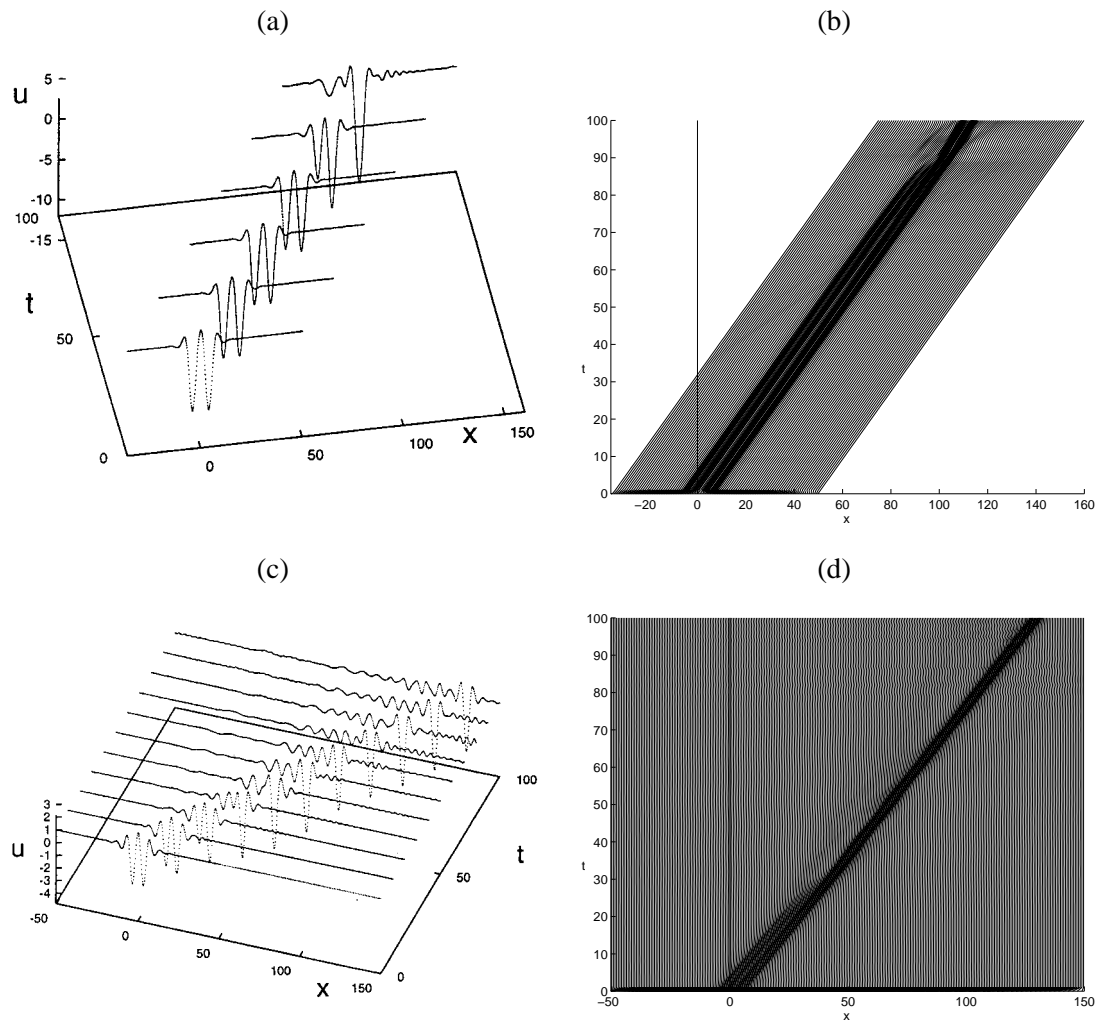


Figure 5. A different instability; (a) Solution and (b) the grid of a moving boundary version of the moving mesh method with *the same* initial data as in Figure 4(a) showing the $\mathbf{2}(2)$ wave for $c = 1.1$ breaking up not by splitting apart but by the two halves of the wave colliding. (c), (d) A similar instability mechanism computed using the moving grid method for the $\mathbf{2}(2)$ wave for $c = 1.3$ using the same initial data as Figure 4b. Both computations used 601 mesh points.

right-hand trough deepens and the two halves of the wave collide leading to a gross break up of the shape of the wave. We also found that running the moving grid method on the data for the $\mathbf{2}(2)$ for $c = 1.3$ (without modification to the moving boundary version this time) also resulted in this ‘collision’ form of instability, see Figures 5c and 5d.

For the case where the $\mathbf{2}(2)$ solitons fission rather than spontaneously break up, the time constant associated with the instability of the $\mathbf{2}(2)$ solution may be gleaned from Figure 6a, which shows the time evolution of the initial data plotted in a moving co-ordinate frame. By comparison, Figure 6b shows a similar instability of the $\mathbf{2}(4)$ wave. Note that the instability of the latter is much slower. This suggests the following conjecture.

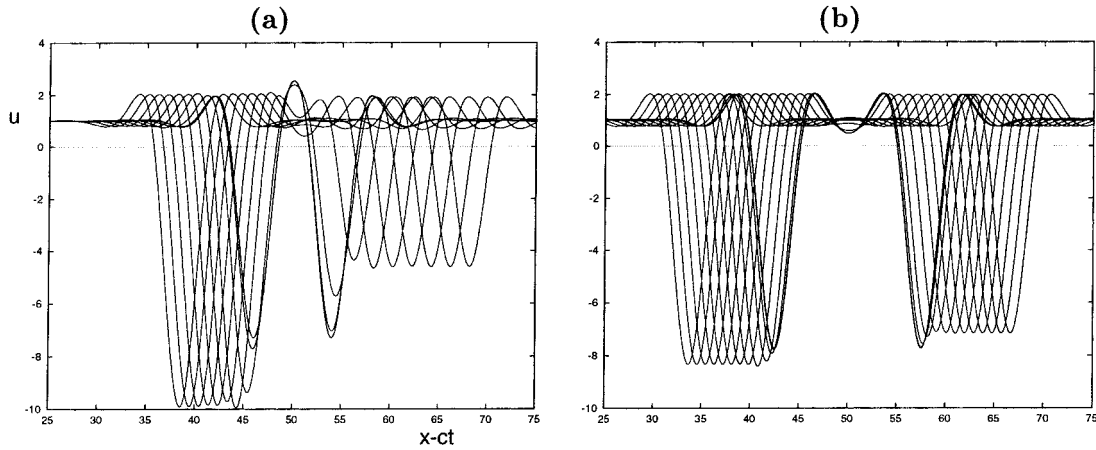


Figure 6. Solutions to Equation (4) using the fixed grid method plotted as u against $x - (1.1)t$ for initial conditions with $c = 1.1$, (a) the $2(2)$ for $t = 0, 20, 40, \dots, 200$ and (b) the $2(4)$ for $t = 0, 60, 120, \dots, 780$.

CONJECTURE 2. *The $2(2m)$ -solutions for $m = 1, 2, 3 \dots$ are all of saddle type with one unstable eigenvalue. The modulus of this eigenvalue decreases with m . Nearby initial conditions are: either attracted to a stable solution composed of two primary waves which move apart; or are attracted to a solution where the two halves of the wave interfere grossly with each other. These two behaviours correspond to opposite components of the unstable eigenvector. One component corresponds (for right travelling waves) to the left-hand trough deepening and hence slowing down compared with the right-hand one, and this leads to fission. The other component corresponds to the right-hand trough deepening and hence being caught up by the left-hand trough, leading to the gross interference.*

4.3. APPROXIMATE COLLISIONLESS INTERACTION OR FUSION OF STABLE WAVES

Since Equation (4) is time-reversible, taking the solutions at the large-time end points of Figures 4 or 6 should result in waves recombining into a two-pulse solitary wave. However, since this wave is unstable, running the solution numerically backwards in time is likely to miss the stable manifold of the $2(2)$ wave and instead the two primary waves will interact with each other in some way. Computations by Chen and McKenna [9] suggest that small amplitude primary waves travelling in opposite directions ($c = 1.40$ and -1.354) can pass through each other without interaction. These computations are repeated and extended in Section 4.5 below.

For the time being, let us investigate the interaction of two primary waves of larger amplitude and travelling with similar wave speeds.

Figure 7a shows the interaction between two primary waves of speeds $c = 1.04$ and $c = 1.2$, which are the approximate wave speeds of the waves that bifurcate from the $2(2)$ solution with $c = 1.1$. Note that at $t \approx 500$ the profile appears to be approaching the $2(2)$ wave but then develops in a quite different manner. Instead of two similar waves emerging on the other side of the interaction, we find that the smaller, faster wave is absorbed by the deeper, slower one. In addition we see apparent numerical noise, which we assume to be ‘radiation’ that has not been fully resolved at this level of numerical discretization.

Figure 7b shows a similar computation with primary solutions having $c = 1.2$ and 1.3 . Again the smaller trough is approximately absorbed by the bigger one. This time there is not

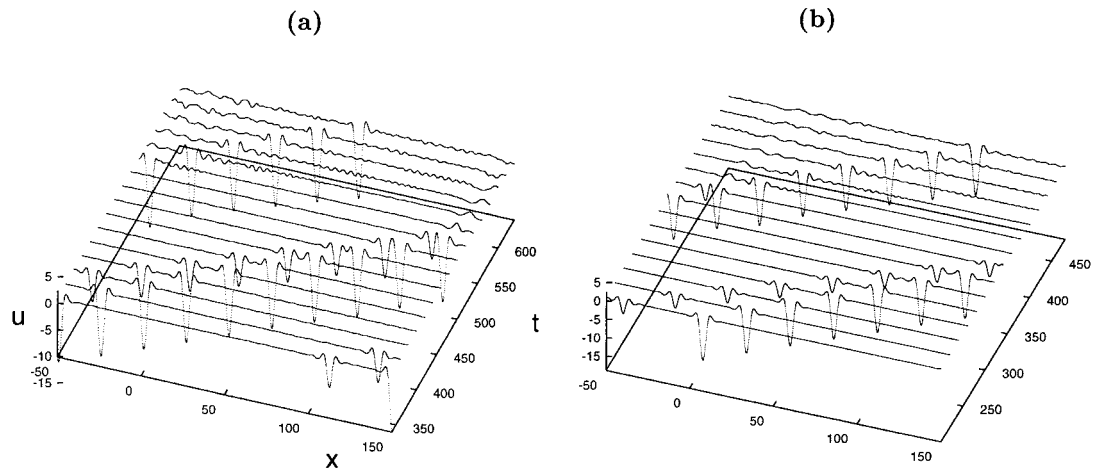


Figure 7. Fusion; when a smaller faster wave catches up with a large slower one, the result may be a single new wave plus some background radiation. This figure shows solutions to Equation (4) with initial conditions composed of the concatenation of two primary solitary waves with different velocities; (a) $c = 1.2$ and 1.04 , (b) $c = 1.2$ and 1.3 .

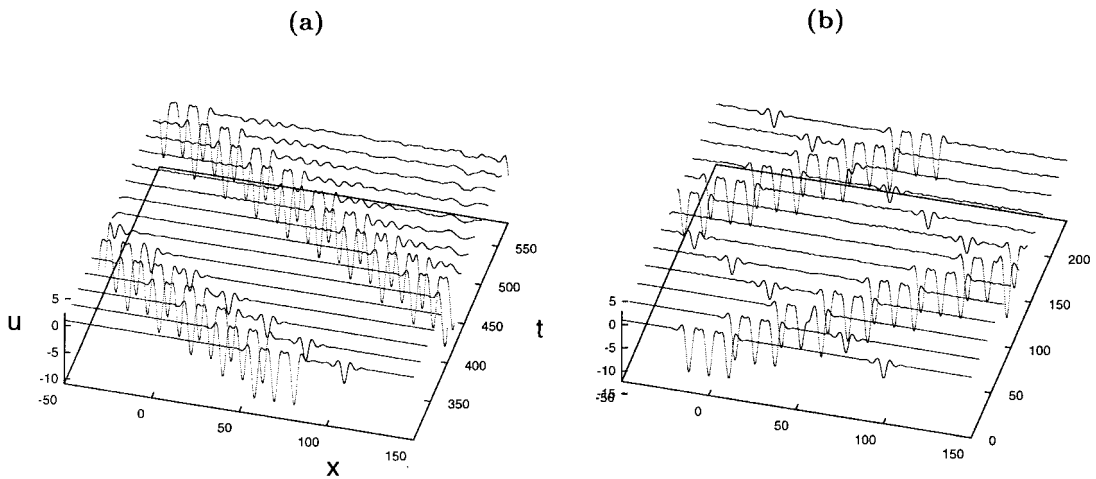


Figure 8. Waves which pass through each other repeatedly with almost no interaction; numerical solutions to Equation (4) using the fixed grid method with initial conditions composed of the concatenation of the primary solitary wave with $|c| = c_1 = 1.3$ and the $3(3, 3, 3)$ with $|c| = c_2 = 1.1$: (a) $\text{sign } c_1 = \text{sign } c_2$, and (b) $\text{sign } c_1 = -\text{sign } c_2$.

so much evidence to suggest that a 2-pulse solution is approached in the interaction. This is not so surprising since there is no evidence to suggest that $c = 1.2$ and 1.3 are the wave speeds created by the fission of a 2-pulse.

Figure 8a shows the results of a similar computation but where the two waves are the primary for $c = 1.1$ and the stable 3-toughed solution depicted in Figure 3b. The results are similar, in that the faster, shallower wave catches up with the slower, deeper one whereupon it is absorbed with the consequent emission of radiation. However, if the same experiment is repeated with the two waves having wave speeds of different signs (note that only c^2 appears

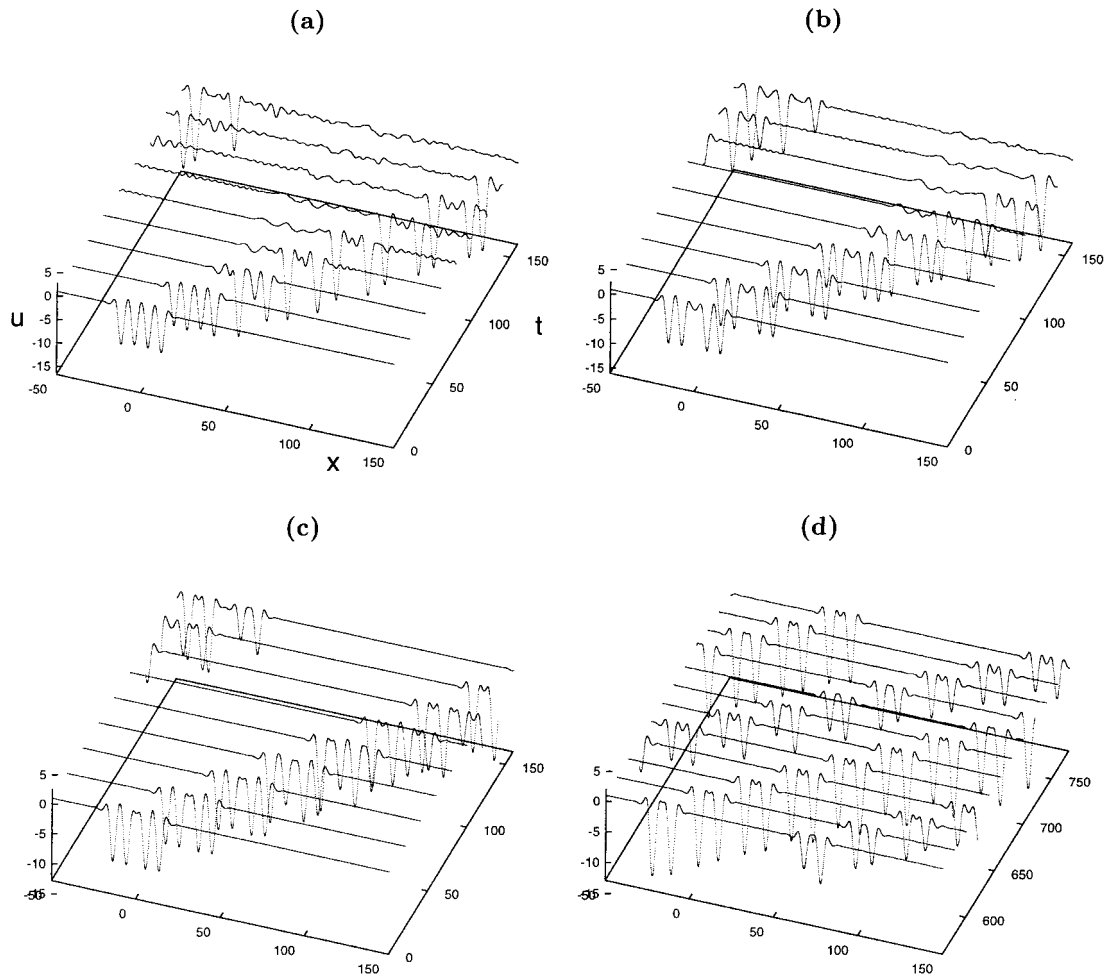


Figure 9. Fission of four-troughed waves; three different outcomes for slightly different waves. Here we see the results for four-troughed solitary waves with $c = 1.1$ (a) the $4(2, 2, 2)$ (b) the $4(2, 4, 2)$ (c) the $4(2, 3, 2)$, (d) the same solution as (c) plotted after a 550 time units.

in the travelling wave ODE (3)) then a very different picture emerges, see Figure 8b. Now the two waves appear to pass through each other with little if any radiation. Since we are using periodic boundary conditions, we can find that the waves repeatedly pass through each other and only after a repeated number of such collisions does there appear to be much 'noise' superimposed on the original data. The first two such collisions are depicted in the figure.

4.4. SOLITARY WAVES WITH MORE THAN TWO TROUGHS

Let us turn our attention now to the dynamics of yet more complex solitary waves. Figure 9 shows the results of time integrations of initial conditions corresponding to four-trough solitary waves with $c = 1.1$ which are composed of two $2(2)$ waves separated by differing numbers of oscillations. Recall that numerical computations suggest the $2(2)$ is itself unstable.

Observe from the figure that we find two distinct modes of instability for these $4(2, n, 2)$ solutions depending on the parity of n . If n is even (Figures 9a and 9b) then we find that the

wave spontaneously breaks into three primary waves together with some radiation. Note that it is harder to distinguish the third primary wave to the right of the two deep trough ones in Figure 9a, because it is of much smaller amplitude and hence is masked by the radiation. The two larger primaries have similar wave speeds and after giving off their radiation appear to be quite stable objects. The presence of radiation may cause us to call this a ‘catastrophic’ instability.

The second form of instability appears when n is odd (see Figure 9c). This instability is of a milder form. There is no spontaneous emission of radiation and the 4-pulse slowly splits into approximately two $\mathbf{2}(3)$ solitary waves with slightly different wave speeds (recall that this 2-pulse wave appears stable). Note however from Figure 9d, which shows the same numerical run at later times, that although these approximate 2-pulses propagate very stably. They do not settle into steady travelling waves. Instead there is a slow mode of oscillation whereby the troughs are of unequal depth and alternatively get larger and smaller than each other. One explanation for this is that each approximate 2-pulse has converged onto the basin of attraction of the $\mathbf{2}(3)$ solitary wave, but owing to fact that time-dependence enters the PDE as a second derivative, the linearization in this basin gives a centre (pure imaginary eigenvalues). Hence the $\mathbf{2}(3)$ is only Liapunov orbitally stable rather than asymptotically. Thus, nearby solutions oscillate about the exact solution in the manner depicted in Figure 9d.

Once again, we need to remember that, in accordance with Conjecture 2 above, any mode of instability will lead to globally very different results depending on whether the initial perturbation in the direction of that mode causes two troughs to be pushed together or pulled apart. (Recall that in our computations this initial perturbation is caused merely by numerical approximation.) This is brought home in Figure 10 which is a moving mesh computation using the same initial data as in Figure 9a. Observe the qualitative difference in the two time histories which is due to the troughs of the initial data colliding or separating in a different order. Note also though that the moving mesh results were robust under an increase in accuracy (changing the number of mesh points).

Now we turn to four-troughed waves which are based on two copies of a two-pulse that appears stable as a solution of the evolutionary problem, namely the $\mathbf{2}(3)$ solution. Figure 11 shows the results of time integrations with initial conditions for the solitary waves with labels $\mathbf{4}(3, i, 3)$, for $i = 1, 2, 3$, again for $c = 1.1$. Note that these waves all behave far more regularly than the $\mathbf{4}(2, i, 2)$ ones depicted in Figure 9. There is no emission of radiation. But once again there is a contrast between the cases where i is even or odd. When i is even, as in Figures 11a and 11b for the $\mathbf{4}(3, 2, 3)$ the solitary wave fissions into simpler stable waves. In this case it splits into two primaries and a $\mathbf{2}(3)$, which then propagate stably for long times. The $\mathbf{4}(3, 4, 3)$ is also unstable but has a much weaker mode of instability, (Figure 11d) and appears to split into only two waves, both of $\mathbf{2}(3)$ type, albeit for different wave speeds. We conclude that to predict *a priori* which stable solitary waves (and indeed their wave speeds) an unstable wave will fission into is a non-trivial task.

Finally we note that the $\mathbf{4}(3, 3, 3)$ wave (Figure 11c) appears completely stable. When plotting all the computed profiles up to $t = 780$ against $x - (1.1)t$ (as in Figure 11d for the $\mathbf{4}(3, 4, 3)$) it was found that all the graphs were overlaid. This result leads us to the following conjecture.

CONJECTURE 3. *Exact solitary wave solutions $\mathbf{n}(i_1, i_2, \dots, i_{n-1})$ of Equation (4) are stable if and only if i_j is odd for all $j = 1, \dots, n - 1$.*

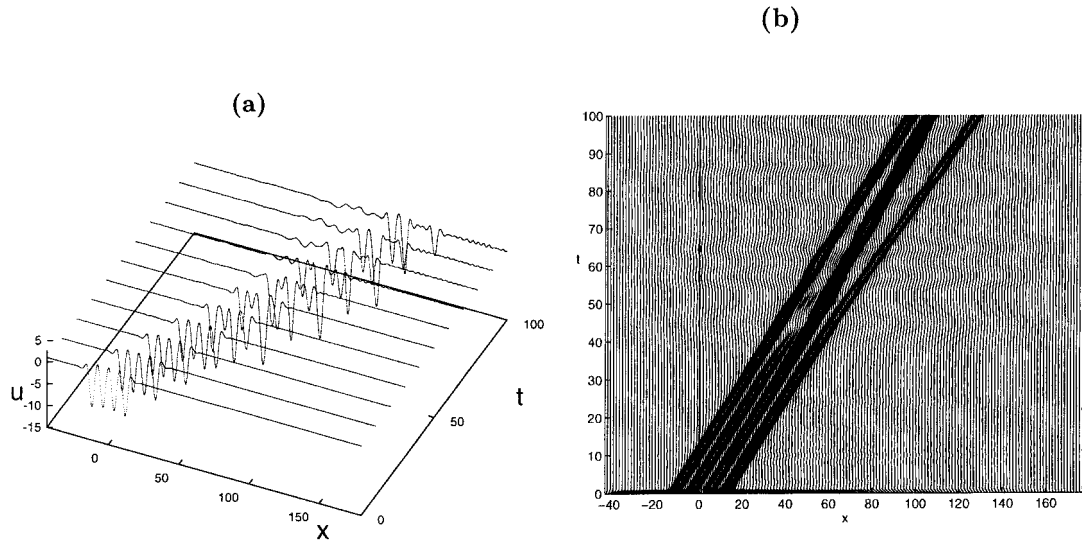


Figure 10. (a) Solution and (b) the moving mesh method for the $\mathbf{4}(2, 2, 2)$ wave using the same initial data as in Figure 4. The data presented is for a run with 1501 grid points, a more accurate run with 2001 produced qualitatively the same results.

For waves which are unstable, we have demonstrated several different mechanisms of instability, including a catastrophic collapse into radiation or a fissioning into simpler stable waves.

4.5. INTERACTION: A COMPARISON BETWEEN PIECEWISE-LINEAR AND EXPONENTIAL NONLINEARITIES

So far, all the time-dependent computations presented have been for the exponential restoring term (4). We have repeated some of the above numerical calculations for the nonlinear term (5) for $\varepsilon = 0.0$ and 0.5 . We find that there are qualitatively no differences in the results for the stability or fission properties of the primary or two-trouged waves.

Figure 12 presents a re-computation of a run in [10] of primary waves travelling towards each other with speeds $|c| = 1.354$ and $|c| = 1.4$. Here we perform such a computation for *both* nonlinearities (2) and (4), and both numerical methods. For both nonlinearities the two methods agree. The results suggest that the exponential nonlinearity gives rise to a radiationless interaction whereas the piecewise-linear term does not. Moreover, using periodic boundary conditions with the fixed grid method, for the exponential nonlinearity, the waves can interact several times without losing shape or generating noise.

Now let us consider the interaction of larger amplitude waves. Figure 13 shows the interaction of two primary waves with equal and opposite initial wave speeds for both the exponential nonlinearity and (5) for $\varepsilon = 0.0$ (i.e., Equation (2)). Note that there is little qualitative difference between the two behaviours, and if anything the radiation seems *more* pronounced in the exponential case. The results for Equation (5) with $\varepsilon = 0.5$ are found to be almost indistinguishable from those in Figure 13a.

One possibility might be that the radiation observed in these ‘collision’ runs is caused by the boundary conditions used. We have investigated this using reflectionless boundary conditions as in [9, 10] and found that they make no qualitative difference. Also, note that

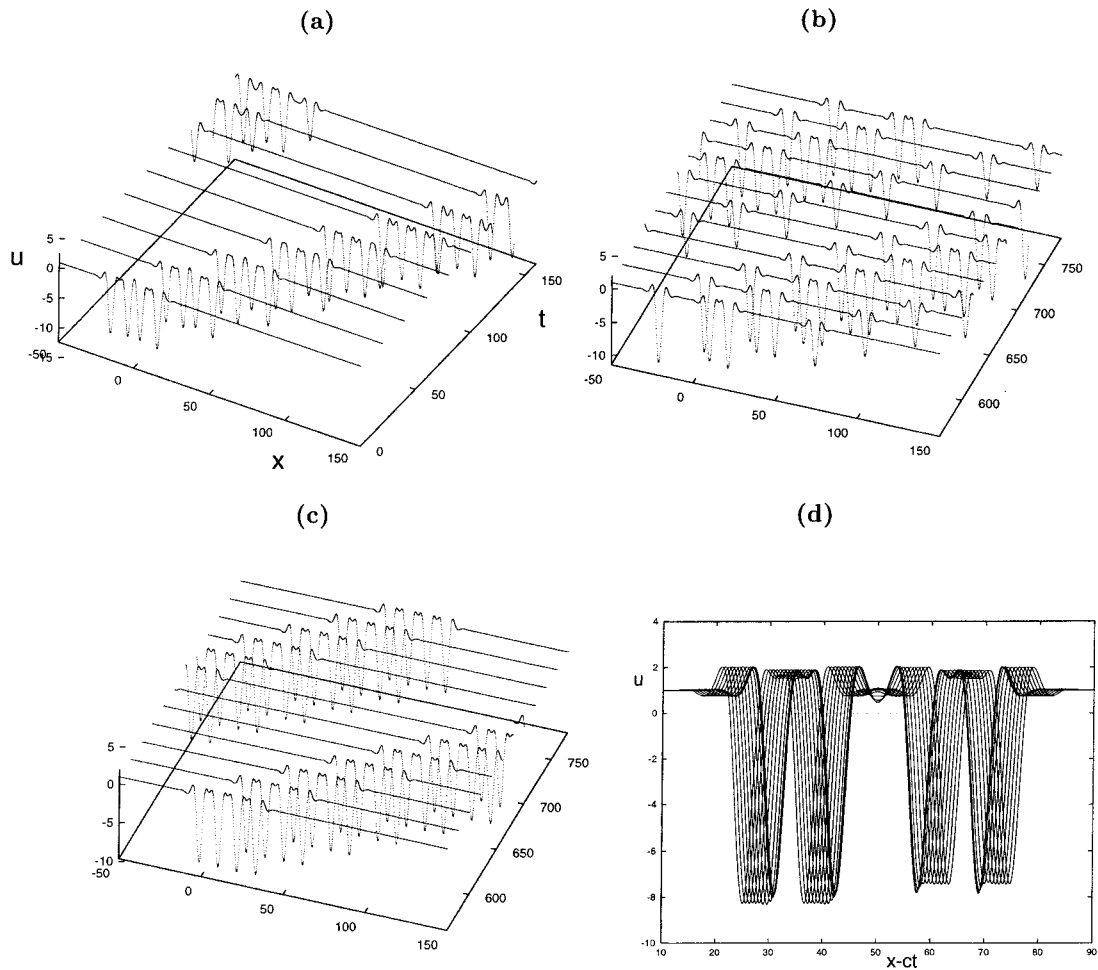


Figure 11. Analogous to Figure 9 but with initial conditions (for $c = 1.1$): (a) the $\mathbf{4}(3, 2, 3)$; (b) the same solution as (a) plotted after 550 time units; (c) the $\mathbf{4}(3, 3, 3)$ plotted after 550 time units; (d) the $\mathbf{4}(3, 4, 3)$ solution plotted against $x - (1.1)t$ for $t = 0, 60, 120, \dots, 780$.

the two numerical methods used in Figures 13b and 13c use different boundary conditions – periodic and zero flux respectively – and that the radiation apparent in the more detailed Figure 13c is clearly initiated at the collision point, *not* at the boundary.

5. Discussion

We have studied a simplified dimensionless model of a suspended beam supported from one side only. Using numerical techniques we have tried to ascertain information on the existence, stability and interaction properties of solitary waves. Let us now collect the various conjectures we made that are suggested by the numerical results

First we have the results on *stability* and *fission* given an initial condition that is close to an exact solitary wave (Conjectures 1–3 above). Given the labeling $\mathbf{n}(m_1, m_2, \dots, m_{n-1})$ of multi-troughed waves introduced in Section 2, then a set of rules appears to emerge by which one can conjecture the stability of the wave from its label (and hence its shape). The first rule

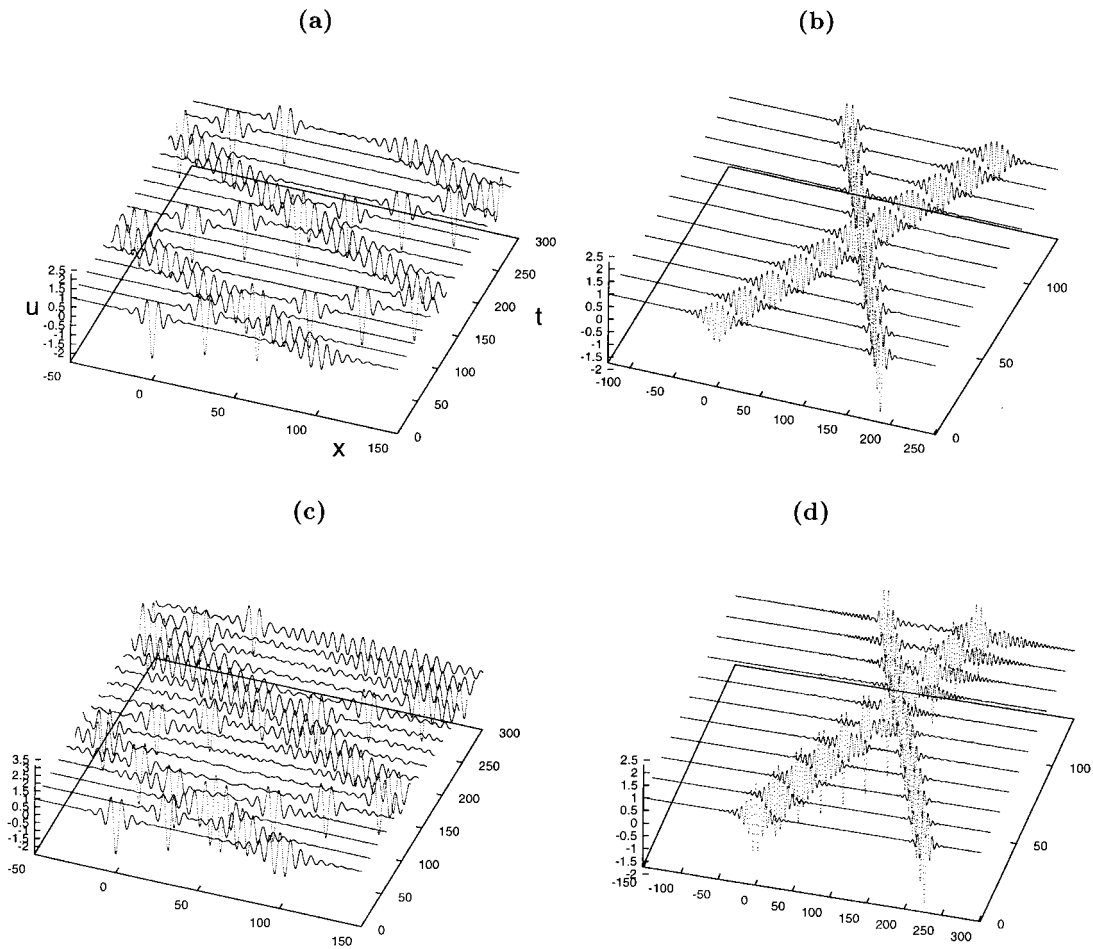


Figure 12. Passage of primary solitary wave solutions to Equation (1) with $|c| = 1.354$ and 1.4 through each other. (a), (b) With the exponential nonlinearity (4), using respectively the fixed and moving grid methods. (c), (d) With the piecewise-linear term (2) using respectively the fixed and moving grid methods. Moving grid computations were performed using 2001 grid points.

is that the wave is stable if and only if all its symbols m_i are odd. The next rule is that if there is an even symbol m_i anywhere in the label then the wave fissions into simpler waves with the possible emission of ‘radiation’. Sometimes this fission is relatively harmless, and the wave slowly splits into two waves with slightly different amplitudes that move *apart* with similar wavespeeds (as in Figures 4, 11b, and 11d).

It seems remarkable that we can have such a spontaneous decomposition of the large more complex ‘heavier’ waves into simpler forms (in a very pure way), while similar close waves (e.g., $2(m)$ waves for which m_i is odd) can remain completely stable. It is tempting to wonder whether such a property may shed some light into mechanisms of how some atoms (large complex localised waves) can decompose whereas ones only slightly different can last indefinitely, something that linear quantum mechanics cannot explain.

Other times, the fission causes a catastrophic destruction into radiation, typically when the difference in amplitude of the splitting waves causes them to travel *towards each other* as in Figure 9a and the left-hand splitting pair of troughs in Figure 9b. Note also that it

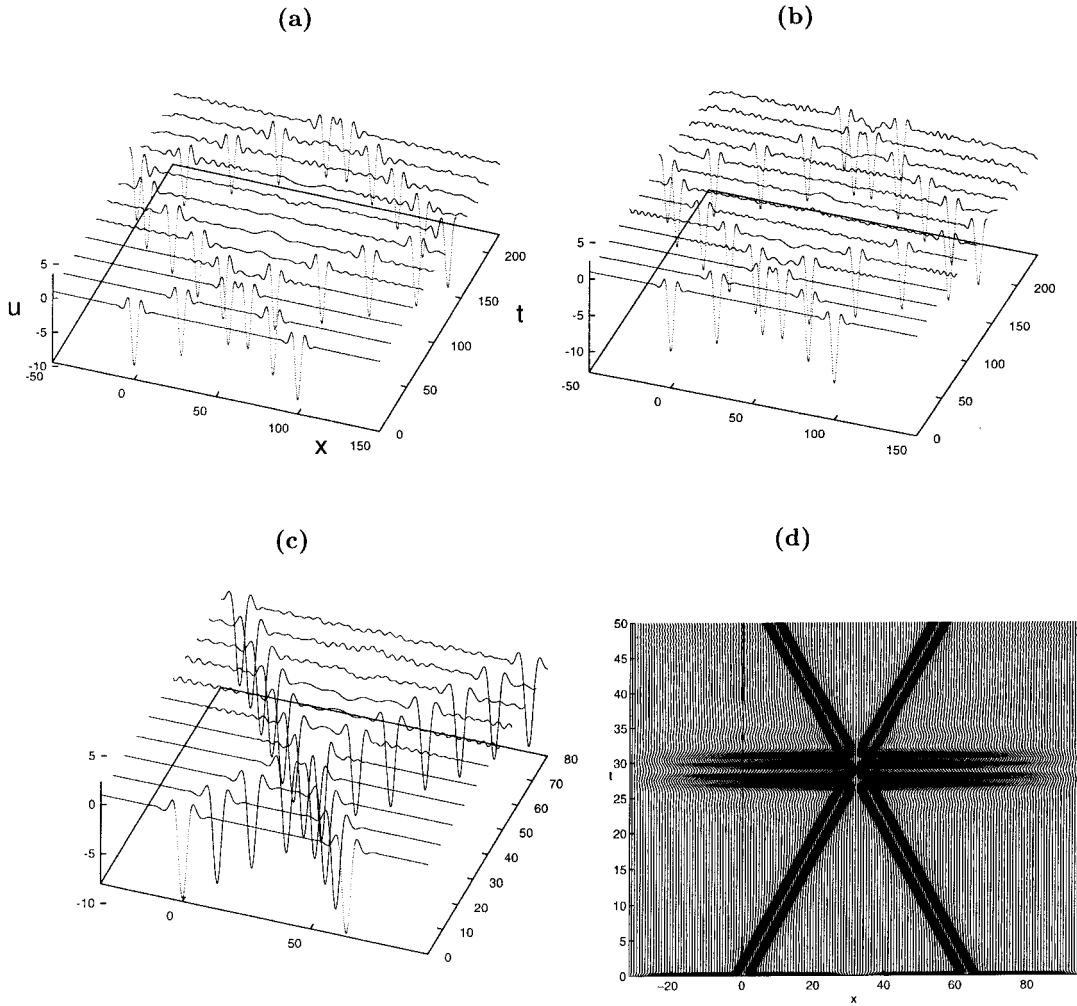


Figure 13. (a) Solution to Equation (1) with the piecewise-linear term (2) using the fixed grid method showing the interaction of two primary waves with initial wave speeds $c = 1.1$ and -1.1 . (b) The equivalent run for the exponential nonlinearity Equation (4). (c) The same run as (b) using the moving grid method with 2001 grid points; and (d) motion of the grid (from a qualitatively identical run with 1001 grid points).

appears from the moving grid computations that it is a function of the perturbation to the unstable waves which decides whether the mild splitting instability or the catastrophic collision instability occurs (e.g., compare Figures 4 and 5). Although most of our computations were for the exponential nonlinearity (4), we have found no evidence to suggest that these (in)stabilities are sensitive to the precise form of the nonlinearity (we have found similar results for Equations (2) and (5)).

The *dynamics* of the *interaction* and possible *fusion* of stable solitary waves seems harder to characterize. A general pattern appears to be that waves with very different speeds (like in Figures 8b and 13) approximately pass through each other with some emission of radiation. In contrast, those with similar wave speeds (as in Figures 7 and 8a) undergo a fusion type process where the smaller amplitude wave is approximately absorbed into the bigger one, again with

added radiation. It is hard via a finite number of numerical experiments to completely satisfy oneself that this radiation is not numerical error.

The most intriguing numerical result is the apparent behaviour for small amplitude stable solitary waves (with $|c|$ close to $\sqrt{2}$), when two waves with velocities of opposite sign are allowed to collide, see Figure 12. It appears that for the exponential nonlinearity (4) two primary waves interact without giving off *any* radiation (up to numerical accuracy) whereas for the piecewise-linear f (2) there appears to be some radiation given off. This caused Chen and McKenna [9, 10] to wonder whether Equation (1) with the particular restoring force term (4) may possess extra structure, akin to completely integrable systems that may give rise to this ‘soliton-like’ collisionless interaction. At present we can give no further insight other to say that we can envisage two possible interpretations of our numerical results. One is that there is no qualitative difference between the nonlinearities, just that for small-amplitude waves (as in Figure 12) the exponential nonlinearity gives rise to quantitatively negligible radiation. The other interpretation is that there really is something special about the exponential nonlinearity and that the radiation for the interacting primary waves with $c = 1.1$ in Figures 13b and 13c is spurious and caused by numerical error. (It should of course be remembered that the three nonlinearities have the same characteristic shape at least for $u < 0$.)

We have tried in this paper to gain a qualitative understanding of the rich dynamics of solitary wave solutions to Equation (1) by performing a finite number of numerical experiments. As with all such attempts, it is possible we are being deceived by numerical error. One thing we can say in defense of the observations we have made is that they appear to be repeatable using two quite different numerical methods. We have presented no analytic results whatsoever. Leaving aside the questions of existence of solitary waves, before closing the paper let us comment on analytical techniques that *may* be of relevance in trying to prove rigorous statements about our numerical observations.

We mention the work of Levandosky [18] for equations of the form (1) (also in higher spatial dimensions) where $f(u) = u - u^{p-1}|u|$ for some integer $p > 0$. (Note that *none* of the nonlinearities considered here fall into that class.) He shows that the ‘ground state’ which we call the primary wave, exists and is stable for some wave speeds.

Sandstede [24] has provided a rigorous framework for proving stability and instability of multi-pulse solutions for a class of PDE systems. That theory gives a similar pattern of alternating stability then instability for two-pulsed solutions parametrised by their label (equivalently the ‘distance between troughs’). At first sight, Equation (1) does not seem to fit into the framework of that paper but nonetheless his technique of analysis may well apply. We also note that Sandstede [25] has applied these techniques to show the *instability* of a homoclinic solutions to a fourth-order equation similar to Equation (3), arising in static buckling problems, but for which the time dependent formulation is very different.

Another context in which travelling waves of a PDE lead to ODEs of the form (3) is for the so-called fifth-order Korteweg–de Vries equation (see [4] for a review). For that equation, which is first order in time, in the appropriate parameter region there are also primary and multi-pulsed solitary wave solutions, and it is known that the primary wave is stable (in an appropriate sense) and that the two-pulses also share the property of alternating stability and instability [3]. Note that this latter paper uses an approximate technique due to Gorkov and Ostrovsky that may well apply to the present equation. We also note the numerical results of Malomed and Vanden-Broeck [20] which show similar approximate interaction with emission of radiation for two stable pulses of that equation.

There are clearly many open questions arising from this paper. We appear to have only scratched the surface of the dynamics of even a small subclass of the solution of this infinite-dimensional nonlinear evolution equation. Nevertheless, we hope that we have captured some of the essential features of the interaction and stability of solitary wave solutions of second-order-in-time nonlinear evolution equations that we are not aware of as being completely integrable. Such systems appear to arise in several distinct applications. For example we mention in closing related numerical experiments by Coleman and Xu [11] on the complex interaction of solitary waves of flexure in rods.

Also we might comment on the original motivation for the PDE; the observation of travelling waves on the Golden Gate suspension bridge. There has been some reticence among engineers to adopt simple qualitative models such as Equation (1) to help understand such phenomena. A particular criticism of Equation (1) with f given by the piecewise-linear term (2) was that solitary waves could only occur if $u < 0$ at some point, corresponding to the cable going slack which would require moderately large deflections from the stable position $u = 1$. One conclusion of the present paper seems to be that any restoring force f that models a one-sided spring (softening for $u < 1$) appears to support stable solitary wave solutions. Moreover if f is smooth (as in Figure 2) then for non-dimensional wavespeeds c close to $\sqrt{2}$ these waves can correspond to *arbitrarily small* deflections from the equilibrium state.

Acknowledgements

PJMCK would like to thank Jiri Horak who performed one of the computations presented in Section 4. ARC is supported by an EPSRC Advanced Fellowship.

References

1. Blom J. G. and Zegeling P. A., 'Algorithm 731: A moving-grid interface for systems of one-dimensional time-dependent partial differential equations', *ACM Transactions in Mathematical Software* **20**(3), 1994, 194–214.
2. Buffoni, B., Champneys, A. R., and Toland J.F., 'Coalescence and bifurcation of a plethora of homoclinic orbits for an Hamiltonian system', *Journal of Dynamics and Differential Equations* **8**, 1996, 221–281.
3. Buryak, A. V. and Champneys, A. R., 'On the stability of solitary waves solutions to the 5th-order KdV equation', *Physics Letters A* **233**, 1997, 58–62.
4. Champneys, A. R., 'Homoclinic orbits in reversible systems and their applications in mechanics, fluids and optics' *Physica D* **112**, 1998, 158–186.
5. Champneys, A. R., 'Homoclinic orbits in reversible systems II: Multi-bumps and saddle-centres', *CWI Quarterly*, 1998, to appear.
6. Champneys, A. R. and McKenna, P. J., 'On solitary waves of a piecewise linear suspended beam model', *Nonlinearity* **10**, 1997, 1763–1782.
7. Champneys, A. R. and Toland, J. F., 'Bifurcation of a plethora of multi-modal homoclinic orbits for autonomous Hamiltonian systems', *Nonlinearity* **6**, 1993, 665–772.
8. Champneys, A. R. and Spence, A., 'Hunting for homoclinic orbits in reversible systems: A shooting technique', *Advances in Computational Mathematics* **1**, 1993, 81–108.
9. Chen, Y. and McKenna, P. J., 'Travelling waves in a nonlinearly suspended beam: theoretical results and numerical observations', *Journal of Differential Equations* **136**, 1997, 325–355.
10. Chen, Y. and McKenna, P. J., 'Travelling waves in a nonlinearly suspended beam: some computational results and four open questions', *Philosophical Transactions of the Royal Society of London A* **355**, 1997, 2175–2184.
11. Coleman, B. D. and Xu, J.-M., 'On the interaction of solitary waves of flexure in elastic rods', *Acta Mechanica* **110**, 1995, 173–182.

12. Doedel, E. J., Champneys, A. R., Fairgrieve, T. R., Kuznetsov, Yu. A., Sandstede, B., and Wang, X. J., 'AUTO97 Continuation and bifurcation software for ordinary differential equations', 1997. Available by anonymous ftp from FTP.CS.CONCORDIA.CA, directory PUB/DOEDEL/AUTO.
13. Gorshkov, K. A. and Ostrovsky, L. A., *Physica D* **3**, 1981, 428–438.
14. Hunt, G. W. and Blackmore, A., 'Principles of localised buckling for a strut on an elastoplastic foundation', *Transactions of the ASME* **63**, 1996, 234–239.
15. Iooss, G. and Pérouème, M. C., 'Perturbed homoclinic solutions in reversible 1 : 1 resonance vector fields', *Journal of Differential Equations* **102**, 1993, 62–88.
16. Lazer, A. C. and McKenna, P. J., 'Abstract: Travelling waves in suspension bridges', in *Proceedings of AMS Annual Meeting*, 1991.
17. Lazer, A. C. and McKenna, P. J., 'Large amplitude periodic oscillations in suspension bridges: Some new connections with nonlinear analysis', *SIAM Review* **32**, 1990, 537–578.
18. Levandosky, S., 'Stability and instability of fourth order solitary waves', *Journal of Dynamics & Differential Equations* **10**, 1998, 151–188.
19. Lin, L. and Adams, G. G., 'Beam on tensionless elastic foundation', *Journal of Engineering Mechanics* **113**, 1986, 542–553.
20. Malomed, B. and Vanden-Broeck, J.-M., 'Solitary wave interactions for the fifth-order KdV equation', *Contemporary Mathematics* **200**, 1996, 133–143.
21. McKenna, P. J. and Walter, W., 'Traveling waves in a suspension bridge', *SIAM Journal on Applied Mathematics* **50**, 1990, 703–15.
22. Peletier, L. A. and Troy, W. C., 'Multibump periodic travelling waves in suspension bridges', *Proceedings of the Royal Society of Edinburgh A* **128**, 1998, 631–659.
23. Petzold, L. R., 'A description of DASSL: A differential/algebraic system solver', in *IMACS Transactions on Scientific Computation*, R. S. Stepleman et al. (eds.), North-Holland, Amsterdam, 1983, pp. 65–68.
24. Sandstede, B., 'Stability of multiple-pulse solutions', *Transactions of the American Mathematical Society* **350**, 1998, 429–472.
25. Sandstede, B., 'Instability of localised buckling modes in a one-dimensional strut model', *Philosophical Transactions of the Royal Society of London A* **355**, 1997, 2083–2097.
26. Woods, P. D., 'Localized buckling and 4th-order equations', Ph.D. Thesis, University of Bristol, 1999.
27. Zegeling, P. A., 'Moving-grid methods for time-dependent partial differential equations', CWI-Tract No. 94, Centre for Mathematics and Computer Science, Amsterdam, 1993.